Kinetic Relationships with Processivity in *Serratia marcescens* Family 18 Glycoside Hydrolases

Anne Grethe Hamre and Morten Sørlie*

Department of Chemistry, Biotechnology and Food Science, Norwegian University of Life Sciences, PO 5003, N-1432 Ås, Norway.

* To whom correspondence should be addressed: Morten Sørlie (morten.sorlie@nmbu.no), Tel.: +47-67232562 and Fax: +47-64965901

Keywords: Glycoside hydrolase; processivity; kinetics; thermodynamics.

Abstract

In nature, recalcitrant polysaccharides such as chitin and cellulose are degraded by glycoside hydrolases (GH) that act synergistically through different modes of action including attack from reducing-end and nonreducing-end (exo-mode) and random (endo-mode) on single polysaccharide chains. Both modes can be combined with a processive mechanim where the GH remain bound to the polysaccharide to perform multiple catalytic steps before dissociation into the solution. In this work, we have determined association rate constants and their activation paramaters for three co-evolved GHs from *Serratia marcescens* (*Sm*ChiA, *Sm*ChiB, and *Sm*ChiC) with an oligomeric substrate. Interestingly, we observe a positive correlation between the association rate constants and processive ability for the GHs. Previously, a positive correlation has been observed between substrate binding affinity and processive ability. *Sm*ChiA with highest processive ability of the three GHs bind with a k_{on} of 11.5 ± 0.2 $\mu M^{-1}s^{-1}$, which is five-fold and 130-fold faster than *Sm*ChiB (less processive) and *Sm*ChiC (nonprocessive), respectively.

1. Introduction

Chitin, an insoluble linear polysaccharide consisting of repeated units of β-1,4-*N*-acetylgucosamine (GlcNAc), is common as a structural polymer in crustaceans, arthropods, fungi, and parasitic nematodes. The GlcNAc units that chitin consists of are rotated 180° relative to each other such that the characteristic *N*-acetyl groups of each pyranose are on opposite sides, making chitiobiose ($(GlcNAc)_2$) the repeating unit. Polymers of chitin are synthesized as crystalline fibrils of hundreds to thousands of monomer units [1]. In α-chitin, the most abundant form of chitin, individual chains display a three-dimensional hydrogen bond arrangement in addition to a stacking of the hydrophobic faces of the carbohydrate rings on top of each other [2, 3]. This makes chitin recalcitrant. Calulations show that the free energy barrier in order to decrystallize an individual chitobiose unit from either the reducing- or the nonreducing end of a chitin crystal is 5.6 kcal/mol while it is 8.0 kcal/mol in the middle of the chain [4].

In nature, chitin is degraded by glycoside hydrolases (GHs) in the enzymatic hydrolysis of glycosidic linkages into chitobiose. The hydrolysis is thought to occur through the synergistic action of GHs that have complementary activities [5, 6]. Endo-acting GHs make random scissions in the middle of the polysaccharide chains, whereas exo-acting GHs mainly target single reducing and nonreducing chain ends. This is often combined with a processive mechanism where processive GHs, both endo- and exo-acting, closely associate with polymer chains and repeatedly cleave glycosidic linkages without dissociating from the crystalline surface, preventing once-detached single chains from reassociating with the insoluble material [7-9]. In 1969, a groundbreaking study by Jaime Monreal and Elwyn T. Reese concluded that *Serratia marcescens* was the most efficient chitin degrader amongst 100 tested microorganisms [10]. *S. marcescens* have a complete chitinolytic machinery with an exo-processive GH acting from the reducing end (*Sm*ChiA), an exo-processive GH acting from the nonreducing end

(*Sm*ChiB), and an endo-nonprocessive GH acting on the middle chains (*Sm*ChiC) (Fig. 1) [11]. In the process of overcoming the decrystallization free energy, several surface exposed aromatic amino acids that bind strongly to individual sugar moieties of the polymer and bring individual polymer chains into the active site are important [12-14]. A fundamental difference between the GHs is that the exo-processive *Sm*ChiA and *Sm*ChiB have nine and eight surface exposed aromatic amino acids, respectively, while the endo-nonprocessive *Sm*ChiC only have four (Fig. 1). In *Sm*ChiA and *Sm*ChiB, such aromatic amino acids in the active sites have shown to be vital for the processive mechanism [15, 16].

In a previous study, we determined the thermodynamic signatures of binding the oligomeric substrate $(GlcNAc)_6$ to the active sites of the *S. marcescens* GHs and observed a positive correlation between binding free energy and processive ability [17]. Here, we have expanded this study by examining the kinetics of $(GlcNAc)_6$ binding to the same GHs where we observe a positive correlation between association rate constants and processive ability.

2. Materials and methods

2.1 Chemicals.

Hexa-*N*-acetylglucosamine was obtained from Megazyme (Wicklow, Ireland). All other chemicals were of analytical grade and purchased from standard manufacturers.

2.2 Protein expression and purification

His_{10}-ChiA-E315Q, His_{10}-ChiB-E144Q, and His_{10}-ChiC-E141Q were overexpressed and purified as described elsewhere [17].

2.3 Stopped flow kinetics

Kinetic experiments to measure fluorescence emission changes on $(GlcNAc)_6$ binding were carried out on a SFM4000 stopped-flow spectrophotometer (Bio-Logic, Seyssinet-Pariset, France) thermostatted at 15, 20, 25, 30, and 37 °C with a Fisherbrand™ Polystat™ Heating Circulator (Fisher Scientific, Hampton, New Hampshire, USA). Trp residues were excited at 295 nm. All GH samples (5 µM after mixing) were prepared in 20 mM potassium phosphate buffer pH 6.0 and were rapidly mixed with six $(GlcNAc)_6$ concentrations in the range 2.5 – 25 µM after mixing. All kinetic data were analyzed using the Bio-Kine32 software (v. 4.74.2).

2.4 Eyring analysis

To obtain the activation parameters for $(GlcNAc)_6$ binding to ChiA-E315Q, ChiB-E144Q, and ChiC-E141Q, two forms of the Eyring equation were used (Equation 1 and Equation 2):

$$\Delta G^* = -RTln(\frac{k_{cat}h}{k_bT}) \qquad \text{Equation 1}$$

$$\ln\left(\frac{k_{cat}}{T}\right) = \ln\left(\frac{k_b}{h}\right) + \frac{\Delta S^*}{R} - \frac{\Delta H^*}{RT} \qquad \text{Equation 2}$$

where k_{cat} is the measured rate of the reaction, ΔG^* is the activation free energy, ΔS^* is the activation entropy, ΔH^* is the activation enthalpy, h is the Plancks constant, k_B is the Boltzmann's constant, R is the gas constant, and T is the absolute temperature. ΔG^* was determined by Equation 3. The determined k_{cat} values were fitted to the linear form of the Eyring equation 2 where the linear regression of the points of the Eyring plot (ln k_{cat}/T vs. $1/T$) was performed using OriginPro 2018 (OriginLab Corporation, Northampton, Massachusetts, USA). ΔH^* was determined from the slope of this line ($-\Delta H^*/R$). $-T\Delta S^*$ was determined from the relationship described in equation 3:

$$\Delta G^* = \Delta H^* - T\Delta S^* \qquad \text{Equation 3}$$

3. Results

3.1 Determination of rate constants for $(GlcNAc)_6$ binding to SmChiA, SmChiB, and SmChiC

To determine the rate of substrate association, the three GHs, at fixed concentrations, were mixed with six different concentrations of $(GlcNAc)_6$ in a stopped-flow experiment. The extent of the reactions were monitored by observation of an increase in the Trp fluorescence with time (Fig. 2). A fit of theoretical data to experimental yielded first order rate constants for the binding interactions. The slope of a plot of the rate constants against the individual $(GlcNAc)_6$ consentrations yielded the second order rate constants (Fig. 3). The results show that *Sm*ChiA has the largest association rate constant (k_{on} = 11.5 ± 0.2 $\mu M^{-1}s^{-1}$) followed by *Sm*ChiB (k_{on} = 2.5 ± 0.1 $\mu M^{-1}s^{-1}$) and *Sm*ChiC (k_{on} = 0.09 ± 0.01 $\mu M^{-1}s^{-1}$) (Table 1).

3.2. Determination of activation parameters

The activation parameters for substrate binding were derived from Eyring analysis of the temperature dependence of the second order rate constants (Table 2 and Fig. 4). For binding to $(GlcNAc)_6$, *Sm*ChiA showed the lowest actication enthalpy change ($\Delta H^{\#}$ = 6.2 ± 1.7 kcal/mol) followed by *Sm*ChiB ($\Delta H^{\#}$ = 9.5 ± 1.2 kcal/mol) and *Sm*ChiC ($\Delta H^{\#}$ = 11.6 ± 0.9 kcal/mol). The latter two displayed favorable activation entropy changes ($-T\Delta S^{\#}$ = –0.65 ± 1.2 kcal/mol and $-T\Delta S^{\#}$ = –0.72 ± 0.9 kcal/mol for *Sm*ChiB and *Sm*ChiC, respectively) while *Sm*ChiA had an unfavorable activation entropy change ($-T\Delta S^{\#}$ = 1.7 ± 1.7 kcal/mol). However, there are no statistically difference in the contribution of the activation entropy change to the activation free energy change for the three GHs. The results suggest that *Sm*ChiA binds substrate faster than *Sm*ChiB and *Sm*ChiC due to more favorable intermolecular binding interactions in the transition state.

4. Discussion

The processive hydrolysis of recalcitrant polysaccharides by processive GHs may be considered to contain as many as six steps [18-20]: 1) adsorption of the GH to the solid polysaccharide surface, 2) positioning of the GH near an accessible free chain end, 3) formation of the Michaelis-complex that may include decrystallizing a single chain from the polysaccharide, 4) catalysis with hydrolysis of the β-glycosidic bond, displacement of product, and sliding of the polymer two sugar moieties to form a new Michaelis complex (repetition of these steps provides a processive mode of action), 5) dissociation of the single polysaccharide chain from the active site of the catalytic domain, and 6) release of the enzyme from the polysaccharide surface into the solution, or repetition of step 2). For steps 2) and 3), it is essential that enzyme residues recognize and orient the substrate through intermolecular interactions. Strong binding of the GH to the substrate is central to achieve this, so central that there is a proportionality between the binding free energy of GHs and processive ability. Payne *et al*. proposed that processive ability is directly linked to the capability of an enzyme to decrystallize a polymer chain from a crystal, quantified by the binding free energy of the enzyme to cello-oligosaccharide substrates as shown for three cellulases through a combination of calculations and experimental work [21]. The mathematical description of the relationship of processive ability with ligand binding free energy through the thermodynamics of chemical equilibrium is shown in Eq. 4 where $\Delta G_r°$ is the binding free energy, R is the gas constant, T is the temperature, P^{intr} is the intrinsic processive ability of the GH, k_{on} is the association rate constant, and k_{cat} is the catalytic rate constant.

$$-\frac{\Delta G_r^o}{RT} = ln\left(\frac{P^{intr}k_{on}}{k_{cat}}\right) \qquad \text{Equation 4}$$

This relationship implies that the most processive enzyme will have a more favorable binding free energy compared to less processive enzymes. Experimental evidences for this relationship has been reported for several systems including the co-evolved GHs of *S. marcescens* (the objects of this study) [17], three co-evolved cellulases from *Thermobifida fusca* [22], as well as for a series of mutants in *Sm*ChiB with varying degree of processivity [13, 23].

Two independent studies with two different techniques have demonstrated that *Sm*ChiA is more processive than *Sm*ChiB (*Sm*ChiC is nonprocessive) [24, 25], while a combined computational and experimental study has concluded that *Sm*ChiA binds stronger to the substrate than *Sm*ChiB [17]. In this work, we show that *Sm*ChiA also binds faster (five-fold) than *Sm*ChiB, and that these processive GHs bind 130-fold and 30-fold faster to the substrate than the nonprocessive *Sm*ChiC. In the proposed six steps described above for GH catalyzed processive hydrolysis of recalcitrant polysaccharides, it is clearly beneficial that the GH displays fast binding to the substrate to promote adsoption on the crystalline surface (Step 1), positioning the substrate and forming the Michaelis complex (Step 2 and 3), form the new Michaelis complex after hydrolysis (Step 4), and preventing the dissociation of the enzyme from dissocation into the solvent (Step 6). In this work, we observe that the most processive of the three GHs from *S. marcescens*, *Sm*ChiA, also has the highest association rate with the substrate followed by *Sm*ChiB, which has the second highest processive ability, while the nonprocessive *Sm*ChiC has a significantly slower association rate than the processive GHs. So, it appears that there is a proportionality between the substrate association rate and processive ability in the same way as there is with substrate affinity. In this regard, it is interesting to examine the differences in the active sites between the GHs. *Sm*ChiA has four strong-binding aromatic amino acids in the active site, in addition to a strong-binding subsite, that interact via hydrogen bonds to the $(GlcNAc)_6$ substrate [13, 26, 27]. *Sm*ChiB and *Sm*ChiC have only three [13, 28] and two [14] strong-binding aromatic amino amino acids in the active site, resepctively.

Moreover, in *Sm*ChiA the aromatic amino acids are on both sides of the catalytic acid (two in negative subsites and two in positive subsites). In *Sm*ChiB, the aromatic amino acids are only in positive subsites, while in *Sm*ChiC only in negative subsites. Several studies show that the processive ability in GHs increases with the number of aromatic amino acids in the active sites and/or the number of loops forming roofs over the active sites [9, 15, 29]. Moreover, it is worth noticing that the relatively slow-binding, nonprocessive *Sm*ChiC has the strongest intermolecular interactions with the substrate when forming the Michaelis-complex (Table XYZ) [17], while the enthalpic penalty in the transition state is the highest compared to the two other GHs. Binding of the substrate to *Sm*ChiC depends more on the formation of hydrogen bonds than stacking interactions between sugar moieties and aromatic amino acids as is observed for *Sm*ChiA [17, 27]. The π electrons of the aromatic residue can form several CH-π interactions with the sugar ring [30], and by this creating a flexible and 'fluid-like' sheath along which the polymer chain can slide in a processive action [29, 31]. The results obtained in this study suggest that such interactions also promotes rapid association of the sugar moieties to the active site. Compared to, for example, hydrogen bonds, hydrophobic stacking interactions are non-specific and involve larger interaction surfaces. This study shows that they apparently also are lowering the enthalpic pentalty of the transition state, which appears to be beneficial for processive ability of GHs.

Acknowledgments

This work was supported by grant from the NorwegianResearch Council (209335).

Reference List

[1] J. Synowiecki, N.A. Al-Khateeb, Production, properties, and some new applications of chitin and its derivatives, Crit.Rev.Food Sci., 43 (2003) 145-171.
[2] P. Sikorski, R. Hori, M. Wada, Revisit of α-chitin crystal structure using high resolution X-ray diffraction data, Biomacromolecules, 10 (2009) 1100-1105.
[3] R. Minke, J. Blackwell, The structure of alpha-chitin, J. Mol. Biol., 120 (1978) 167-181.
[4] G.T. Beckham, M.F. Crowley, Examination of the α-chitin structure and decrystallization thermodynamics at the nanoscale, J. Phys. Chem. B, 115 (2011) 4516-4522.
[5] B. Henrissat, H. Driguez, C. Viet, M. Schulein, Synergism ofcellulases from Trichoderma reesei in the degradation of cellulose, Bio-Technology, 3 (1985) 722-726.
[6] S. Merino, J. Cherry, Progress and challenges in enzyme development for biomass utilization, Adv. Biochem. Eng. Biotechnol., 108 (2007) 95-120.
[7] G.T. Beckham, J. Ståhlberg, B.C. Knott, M.E. Himmel, M.F. Crowley, M. Sandgren, M. Sørlie, C.M. Payne, Towards a molecular-level theory of carbohydrate processivity in glycoside hydrolases, Curr. Opin. Struct. Biol., 27 (2014) 96-106.
[8] T.T. Teeri, Crystalline Cellulose Degradation: New Insight into the Function of Cellobiohydrolases, Trends Biotechnol., 15 (1997) 160-167.
[9] I. von Ossowski, J. Stahlberg, A. Koivula, K. Piens, D. Becker, H. Boer, R. Harle, M. Harris, C. Divne, S. Mahdi, Y. Zhao, H. Driguez, M. Claeyssens, M.L. Sinnott, T.T. Teeri, Engineering the Exo-loop of Trichoderma reesei Cellobiohydrolase, Cel7A. A comparison with Phanerochaete chrysosporium Cel7D, J.Mol.Biol., 333 (2003) 817-829.
[10] J. Monreal, E.T. Reese, Chitinase of *Serratia marcescens* Can. J. Microbiol., 15 (1969) 689-696.
[11] G. Vaaje-Kolstad, S.J. Horn, M. Sørlie, V.G.H. Eijsink, The chitinolytic machinery of Serratia marcescens – a model system for enzymatic degradation of recalcitrant polysaccharides, FEBS J., 280 (2013) 3028-3049.
[12] A.G. Hamre, E.E. Frøberg, V.G.H. Eijsink, M. Sørlie, Thermodynamics of Tunnel Formation upon Substrate Binding in a Processive Glycoside Hydrolase, Arch. Biochem. Biophys., 620 (2017) 35-42.
[13] S. Jana, A.G. Hamre, P. Wildberger, M.M. Holen, V.G.H. Eijsink, G.T. Beckham, M. Sørlie, C.M. Payne, Aromatic-mediated Carbohydrate Recognition in Processive *Serratia Marcescens* Chitinases, J. Phys. Chem. B, 120 (2016) 1236-1249.
[14] C.M. Payne, J. Baban, S.J. Horn, P.H. Backe, A.S. Arvai, B. Dalhus, M. Bjørås, V.G.H. Eijsink, M. Sørlie, G.T. Beckham, G. Vaaje-Kolstad, Hallmarks of processivity in glycoside hydrolases from crystallographic and computational studies of the Serratia marcescens chitinases, J. Biol. Chem., 287 (2012) 6322–36330.
[15] S.J. Horn, P. Sikorski, J.B. Cederkvist, G. Vaaje-Kolstad, M. Sørlie, B. Synstad, G. Vriend, K.M. Vårum, V.G.H. Eijsink, Costs and benefits of processivity in enzymatic degradation of recalcitrant polysaccharides, Proc. Natl. Acad. Sci. U.S.A., 103 (2006) 18089-18094.
[16] H. Zakariassen, B.B. Aam, S.J. Horn, K.M. Vårum, M. Sørlie, V.G.H. Eijsink, Aromatic Residues in the Catalytic Center of Chitinase A from *Serratia Marcescens* affect Processivity, Enzyme Activity, and Biomass Converting Efficiency, J. Biol. Chem., 284 (2009) 10610-10617.
[17] A.G. Hamre, S. Jana, M.M. Holen, G. Mathiesen, P. Väljamäe, C.M. Payne, M. Sørlie, Thermodynamic Relationships with Processivity in *Serratia marcescens* Family 18 Chitinases, J. Phys. Chem. B, 119 (2015) 9601-9613.
[18] P. Bansal, M. Hall, M.J. Realff, J.H. Lee, A.S. Bommarius, Modeling Cellulase Kinetics on Lignocellulosic Substrates, Biotechnol. Adv., 27 (2009) 833-848.

[19] E. Praestgaard, J. Elmerdahl, L. Murphy, S. Nymand, K.C. McFarland, K. Borch, P. Westh, A Kinetic Model for the Burst Phase of Processive Cellulases, FEBS J., 278 (2011) 1547-1560.
[20] G.T. Beckham, J. Ståhlberg, B.C. Knott, M.E. Himmel, M.F. Crowley, M. Sandgren, M. Sørlie, C.M. Payne, Towards a Molecular-Level Theory of Carbohydrate Processivity in Glycoside Hydrolases, Curr. Opin. Biotechnol., 27 (2014) 96-106.
[21] C.M. Payne, W. Jiang, M.R. Shirts, M.E. Himmel, M.F. Crowley, G.T. Beckham, Glycoside Hydrolase Processivity is Directly Related to Oligosaccharide Binding Free Energy, J. Am. Chem. Soc., 135 (2013) 18831-18839.
[22] A.G. Hamre, A. Kaupang, C.M. Payne, P. Vâljamäe, M. Sørlie, Thermodynamic signatures of substrate binding for three Thermobifida fusca cellulases with different modes of action, Biochemistry, 58 (2019) 1648−1659.
[23] S. Jana, A.G. Hamre, V.G.H. Eijsink, M. Sørlie, C.M. Payne, Polar residues lining the binding cleft of a Serratia marcescens family 18 chitinase position the substrate for attack and stabilize associative interactions, Mol. Phys., (2019) 1-19.
[24] A.G. Hamre, S.B. Lorentzen, P. Väljamäe, M. Sørlie, Enzyme Processivity changes with the Extent of Recalcitrant Polysaccharide Degradation, FEBS Lett., 588 (2014) 4620-4624.
[25] K. Igarashi, T. Uchihashi, T. Uchiyama, H. Sugimoto, M. Wada, K. Suzuki, S. Sakuda, T. Ando, T. Watanabe, M. Samejima, Two-way traffic of glycoside hydrolase family 18 processive chitinases on crystalline chitin, Nat. Commun., 5 (2014).
[26] A.L. Norberg, A.I. Dybvik, H. Zakariassen, M. Mormann, J. Peter-Katalinic´, V.G.H. Eijsink, M. Sørlie, Substrate positioning in chitinase A, a processive chito-biohydrolase from *Serratia marcescens*, FEBS Lett., 585 (2011) 2339-2344.
[27] Y. Papanikolau, G. Prag, G. Tavlas, C.E. Vorgias, A.B. Oppenheim, K. Petratos, High resolution structural analyses of mutant chitinase A complexes with substrates provide new insight into the mechanism of catalysis, Biochemistry, 40 (2001) 11338-11343.
[28] D.M.F. van Aalten, D. Komander, B. Synstad, S. Gåseidnes, M.G. Peter, V.G.H. Eijsink, Structural insights into the catalytic mechanism of a family 18 exo-chitinase, Proc. Natl. Acad. Sci. U.S.A, 98 (2001) 8979-8984.
[29] A. Varrot, T.P. Frandsen, I. von Ossowski, V. Boyer, S. Cottaz, H. Driguez, M. Schulein, G.J. Davies, Structural Basis for Ligand Binding and Processivity in Cellobiohydrolase Cel6A from *Humicola Insolens*, Structure, 11 (2003) 855-864.
[30] M. Nishio, M. Hirota, Y. Umezwa, The CH/p Interaction: Evidence, Nature, and Consequences, Wiley, New York, 1998.
[31] W.A. Breyer, B.W. Mattthews, A structural basis for processivity, Prot. Sci., 10 (2001) 1699-1711.
[32] S.J. Horn, M. Sørlie, G. Vaaje-Kolstad, A.L. Norberg, B. Synstad, K.M. Vårum, V.G.H. Eijsink, Comparative studies of chitinases A, B and C from Serratia marcescens Biocatal. Biotransfor., 24 (2006) 39-53.
[33] A. Perrakis, I. Tews, Z. Dauter, A.B. Oppenheim, I. Chet, K.S. Wilson, C.E. Vorgias, Crystal structure of a bacterial chitinase at 2.3 A resolution, Structure., 2 (1994) 1169-1180.
[34] D.M.F. van Aalten, B. Synstad, M.B. Brurberg, E. Hough, B.W. Riise, V.G.H. Eijsink, R.K. Wierenga, Structure of a two-domain chitotriosidase from Serratia marcescens at 1.9-angstrom resolution, Proc.Natl.Acad.Sci.U.S.A, 97 (2000) 5842-5847.

Table 1. Association and dissociation rate constants and processive ability for *Sm*ChiA, *Sm*ChiB, and *Sm*ChiC at t = 30 °C, pH 6.0

Enzyme	k_{on}[a]	k_{off}[b]	P^{app}, [c]	velocity[d]	processivity[d] half-life
*Sm*ChiA	11.5 ± 0.2	6.4	30.1 ± 1.5	70.5 ± 25.2	21
*Sm*ChiB	2.5 ± 0.1	0.52	24.3 ± 2.0	46.9 ± 19.8	13
*Sm*ChiC	0.09 ± 0.01	0.0009	n.a.[e]	n.a.[e]	n.a[e]

[a] $\mu M^{-1}s^{-1}$, [b] s^{-1} (calculated from $k_{off} = k_{on}/K_a$), [c] from Hamre *et al.* [24], [d] speed of chitin degradation in nm s^{-1} from Igarashi *et al*. [25], [e] not applicable, *Sm*ChiC is nonprocessive.

Table 2. Activation parameters and thermodynamic parameters for $(GlcNAc)_6$ binding to *Sm*ChiA, *Sm*ChiB, and *Sm*ChiC at t = 30 °C, pH 6.0

Enzyme	ΔG^{*a}	ΔH^{*a}	$-T\Delta S^{*a}$	$\Delta G_r^{\circ a,b}$	$\Delta H_r^{\circ a,b}$	$-T\Delta S_r^{\circ a,b}$	$\Delta G_r^{\circ a,c}$
*Sm*ChiA	8.0 ± 0.1	6.2 ± 1.7	1.7 ± 1.7	–8.7 ± 0.1	–4.5 ± 0.2	–4.2 ± 0.2	–15.1
*Sm*ChiB	8.9 ± 0.1	9.5 ± 1.2	–0.65 ± 1.2	–9.3 ± 0.1	–0.1 ± 0.3	–9.2 ± 0.3	–13.4
*Sm*ChiC	10.9 ± 0.1	11.6 ± 0.9	–0.72 ± 0.9	–9.7 ± 0.1	–7.8 ± 0.2	–1.9 ± 0.2	–9.6

[a] kcal/mol, derived from the use of isothermal titration calorimetry [17], derived from FEP/λ-REMD calculations and $(GlcNAc)_6$ occupancy in the active site [17, 32].

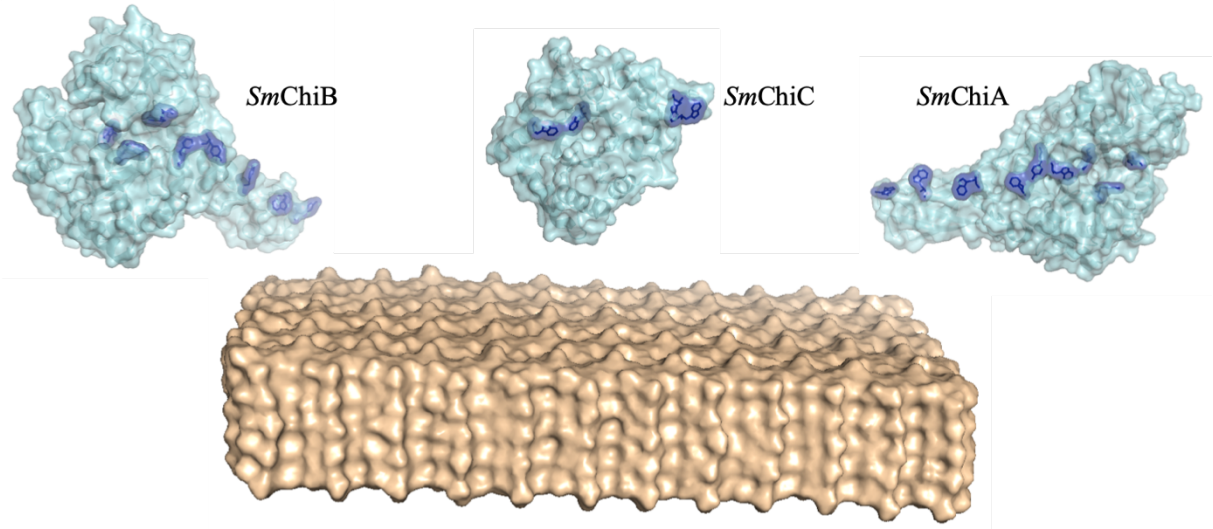

Fig. 1. Crystal structures of *Sm*ChiA (pdb 1ctn [33]), *Sm*ChiB (pdb 1e15 [34]), and *Sm*ChiC (pdb 4axn [14]) of *S. marcescens*. Highlighted in blue are the surface exposed aromatic amino acids that has been shown to be important for substrate binding and processive ability.

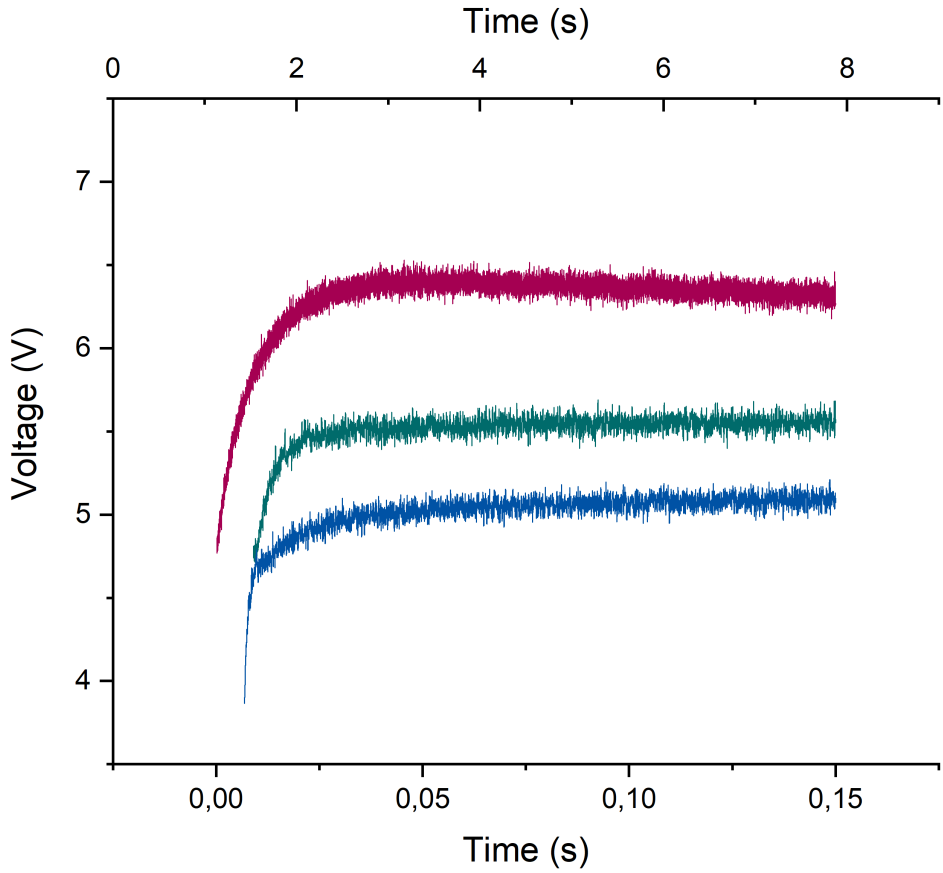

Fig. 2. Time course for the binding of 18 µM $(GlcNAc)_6$ to 5 µM ChiA-E315Q (green), ChiB-E144Q (blue), and ChiC-E141Q (pink) at 30 °C. The lower x-axis belongs to ChiA-E315Q and ChiB-E144Q, while the upper x-axis belongs to ChiC-E141Q.

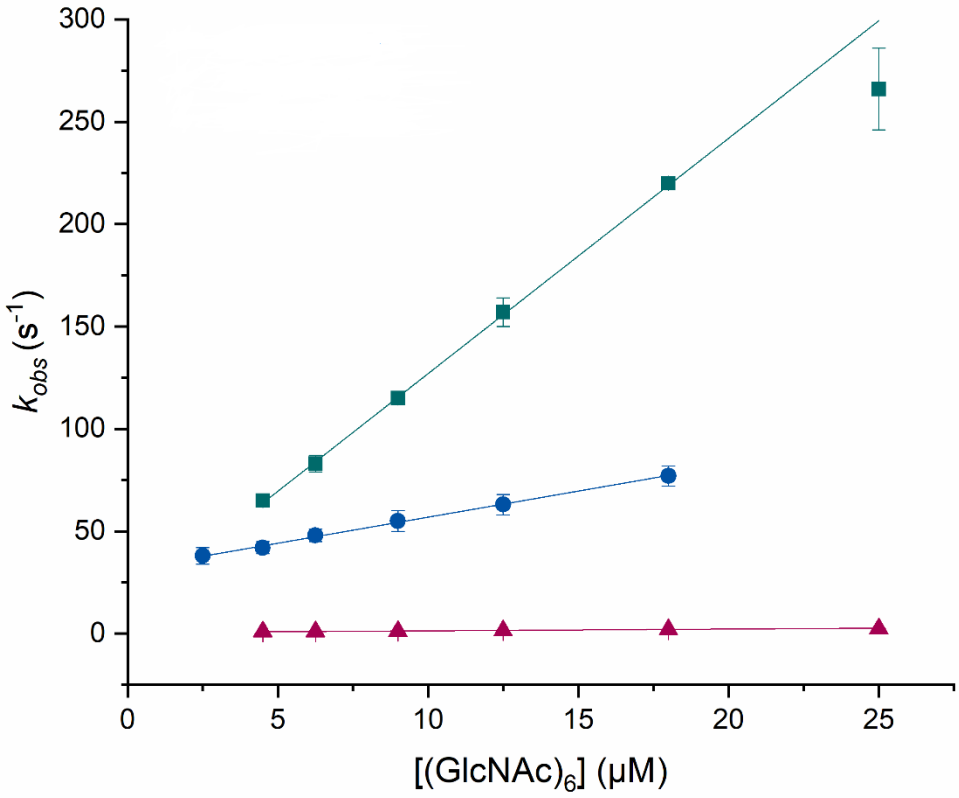

Fig. 3. First-order rate constants for $(GlcNAc)_6$ binding to ChiA-E315Q (green squares), ChiB-E144Q (blue circles), and ChiC-E141Q (pink triangles) as a function of $[(GlcNAc)_6]$ in 20 mM potassium phosphate buffer pH 6.0 at 30 °C.

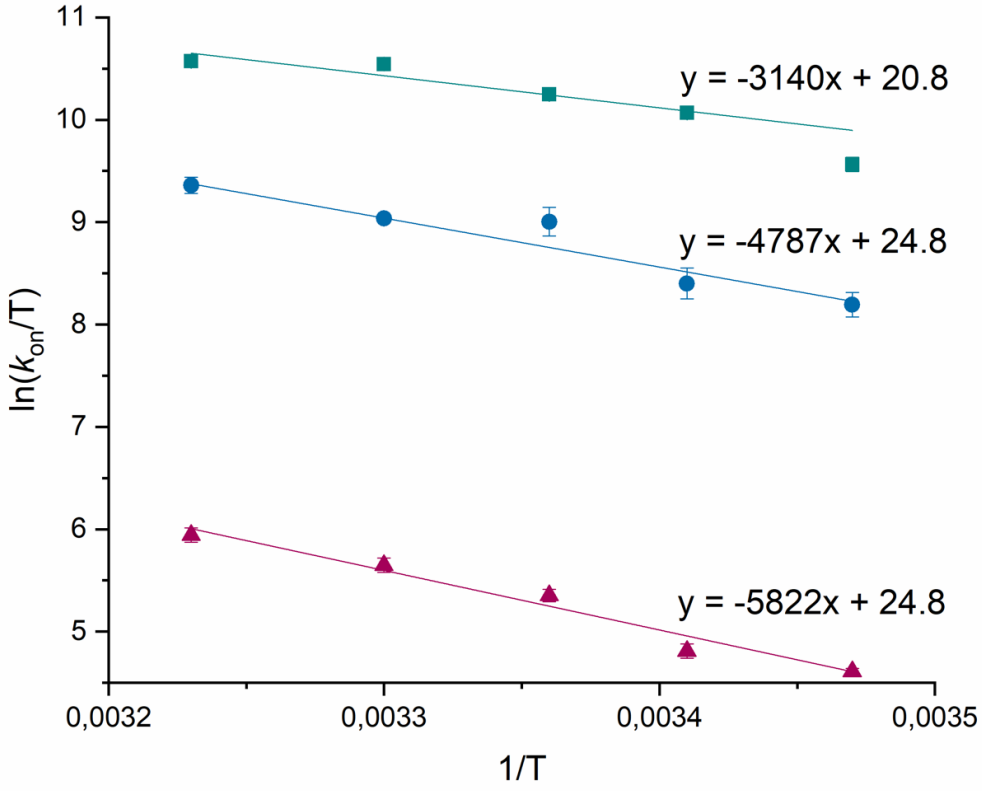

Fig. 4. Eyring-plot for $(GlcNAc)_6$ binding to ChiA-E315Q (green squares), ChiB-E144Q (blue circles), and ChiC-E141Q (pink triangles).